FEBS Letters

journal homepage: www.FEBSLetters.org

Diminished AMPK signaling response to fasting in thioredoxin-interacting protein knockout mice

Allen M. Andres [a], Eric P. Ratliff [a], Sowbarnika Sachithanantham [a], Simon T. Hui [a,b,*]

[a] Department of Biology, BioScience Center, San Diego State University, San Diego, CA 92182, USA
[b] Division of Cardiology, Department of Medicine, University of California, Los Angeles, CA 90095, USA

ABSTRACT

Thioredoxin-interacting protein (Txnip) knockout (TKO) mice exhibit impaired response to fasting. Herein, we showed that activation of adenine monophosphate-activated protein kinase and cellular AMP levels were diminished in the heart and soleus muscle but not in gastrocnemius muscle of fasting TKO mice. Similarly, glycogen content in fasted TKO mice was increased in oxidative muscles but was not different in glycolytic muscles. These data suggest Txnip deficiency has a higher impact on oxidative muscle than glycolytic muscles and provide new insights into the metabolic role of Txnip.
© 2011 Federation of European Biochemical Societies. Published by Elsevier B.V. All rights reserved.

1. Introduction

The ability to make proper adaptive biochemical and physiological changes in response to nutritional status is vital to the survival of all living organisms. Hence, the balance of metabolic fuel utilization is tightly regulated and coordinated. Disruption of this intricate balance is manifested in many common diseases in Western societies, such as obesity and diabetes. Previously, we and others showed that thioredoxin-interacting protein (Txnip) knockout (TKO) mice were unable to respond properly to energy deprivation [1–5]. Prolonged starvation resulted in the death of 90% TKO mice within 72 h while acute fasting led to profound alternations in the plasma metabolic profile of TKO mice which become hypoglycemic, hyperketonemic and hypertriglyceridemic. Surprisingly, although the liver plays a central role in fuel adaptation, liver-specific TKO mice do not have any overt metabolic abnormalities [4]. On the other hand, cardiac and skeletal muscle-specific TKO mice recapitulate the fasting plasma metabolic profile of whole body TKO mice, indicating that the metabolic perturbations by Txnip ablation are mainly due to its loss of function in the heart and skeletal muscle [4]. Mitochondrial oxidation of glucose, fatty acids and ketone bodies in skeletal muscles was found to be reduced in TKO mice, whereas glucose uptake and glycolysis were increased [4].

Txnip is a 46 kDa ubiquitously expressed protein which is involved in maintaining cellular redox rheostat through its disulfide interaction with thioredoxin-1 [6,7]. It is an important metabolic regulator in controlling glucose homeostasis [1,4,5,8,9]. Elevated glucose levels induce Txnip expression [10–12]. Conversely, Txnip expression suppresses glucose uptake and utilization [8,13]. Txnip mutations are linked to lower plasma glucose in type 2 diabetic patients who have elevated levels of Txnip in the pancreatic β-cells [8,13].

Adenine monophosphate-activated protein kinase (AMPK) is the master energy senor in the cell and orchestrates fasting-specific metabolic responses (review in [14]). Activation of AMPK by increased cellular AMP levels inhibits anabolic pathways and promotes catabolic processes to restore ATP levels. Given the central role of AMPK in energy sensing and maintaining energy homeostasis, we investigated the possible link of Txnip ablation in skeletal and cardiac muscles to AMPK signaling and glucose homeostasis.

2. Materials and methods

2.1. Animal studies

Generation of TKO mice was described previously [4]. All studies were performed on overnight fasted mice except where

---

otherwise stated. All procedures described were approved by the Institutional Animal Care and Use Committee at San Diego State University and University of California at Los Angeles.

2.2. Isolation of total RNA and quantitative real-time PCR

Total RNA was isolated from frozen tissue samples using the PerfectPure RNA Isolation Kit (5-Prime). cDNA was generated using iScript cDNA Synthesis Kit (BioRad). Quantitative real-time PCR was performed using the SensiMix Plus SYBR Green Kit (Quantace) on the iCycler system (BioRad). Primers used for GLUT1 mRNA expression were 5′-ggtgtgcagcagcctgtgta-3′ (forward) and 5′-aac aaacagcgacaccacagt-3′ (reverse). GLUT1 expression levels were normalized to that of cyclophilin. Primer sequences for cyclophilin were 5′-tggagagcaccaagacagaca-3′ (forward) and 5′-tgccggagtcga caatgat-3′ (reverse).

2.3. Western blotting

Tissues were homogenized in ice-cold buffer containing 50 mM Tris, pH 8, 150 mM NaCl, 2 mM EGTA, 1 mM EDTA, 1% NP-40, 0.5% sodium deoxycholate, 0.1% SDS, 20 mM NaF, 1 mM $NaVO_4$, 1 mM PMSF, 10 μg/ml aprotinin, 10 μg/ml leupeptin and 10 μg/ml pepstatin. Anti-tubulin antibody was purchased from Sigma. Anti-pPDH-E1α (Ser-293) was purchased from Calbiochem. Antibodies for liver kinase B1 (LKB1), GLUT1 and GLUT4 were purchased from Santa Cruz Biotechnology. All other primary antibodies were purchased from Cell Signaling Technology.

2.4. 5-Aminoimidazole-4-carboxyamide ribonucleoside (AICAR) treatment

Overnight fasted mice were given a subcutaneous injection of AICAR (0.5 mg/g body weight). Control animals received saline only. One hour after injection, mice were sacrificed and soleus muscles were processed for Western blot analysis.

2.5. AMPK activity assay

Tissue were homogenized in Buffer A (50 mM Tris–HCl, 1 mM EDTA, 1 mM EGTA, 1 mM DTT, 50 mM NaF, 5 mM sodium pyrophosphate, 10% glycerol, 1% TritonX-100, pH 7.50) in the presence of protease inhibitor cocktail (Pierce). The homogenate was centrifuged for 15 min at $13\,500{\times}g$. AMPK activity was determined using SAMS peptide as a substrate in the presence of 200 μM AMP as described [15]. The standard assay mixture (in 25 μl) contains 40 mM HEPES (pH 7.0), 80 mM NaCl, 8% glycerol (v/v), 5 mM MgCl, 0.8 mM EDTA, 0.8 mM dithiothreitol, 0.2 mM ATP, 0.2 mM AMP, 0.2 mM SAMS peptide and 2 μCi [^{32}P]ATP (cat #35001X, ICN). After 20 min at 30 °C, the reaction was terminated by spotting 15 μl of reaction mixture onto Whatman P81 paper, which was then washed 5 times in 1% phosphoric acid and once in acetone. The papers were air-dried and radioactivity was quantitated in 4 ml scintillation fluid. Activities of each sample were corrected from no-enzyme controls and normalized to the amount of protein.

2.6. Quantification of tissue nucleotides

Assay of nucleotides levels were performed by the NIH Mouse Metabolic Phenotyping Center at the Yale University School of Medicine. Tissues were snap-frozen in liquid nitrogen. Frozen tissues (50–100 mg) were extracted with 0.9 N ice-cold perchloric acid. The concentrations of ATP, ADP, and AMP in the supernatant were determined by LC/MS.

2.7. Tissue glycogen content

Frozen tissues (20–50 mg) were dissolved in 1 N KOH for 20 min at 65 °C and treated with activated amyloglucosidase (Sigma) in an acidic buffer overnight at room temperature. Samples were then neutralized with 1 N NaOH and assayed using a glucose kit (Wako). Tissue glycogen content is expressed as the amount free glycosyl units (μmol)/g tissue.

2.8. Subcellular fractionation

For LKB1 measurements, cytosolic and nuclear fractions were prepared as described [16]. For GLUT4 analysis, tissues from overnight fasted mice were subfractionated as described [17] with minor modifications. The final pellet was resuspended in buffer containing 30% sucrose and subject to centrifugation ($216\,000{\times}g$) for 1 h at 4 °C to separate the intracellular membranes from the plasma membranes. GLUT4 protein levels were determined in the membrane fractions by Western blotting.

2.9. Measurement of plasma insulin

Plasma insulin levels of fasted and non-fasted animals were determined by the Mouse Insulin Lincoplex kit from Millipore.

2.10. Measurement of 2-deoxyglucose uptake

Deoxyglucose uptake in soleus from overnight fasted mice was determined as described [18]. Soleus muscle from overnight fasted mice was pre-incubated in oxygenated Krebs-Henseleit Buffer (KHB) without insulin for 30 min. Muscles were then incubated for 20 min. in KHB containing 1 mM 2-deoxy-D-[l,2-^{3}H]glucose (2.25 μCi/ml), 0.3 μCi/ml [U-^{14}C]mannitol, 2 mM sodium pyruvate and 0.1% BSA. Tissue was blotted dry and digested in Tissue Solubilizer (ICN). Radioactivity was determined by scintillation counting in the presence of 10 ml Cytoscint (Fisher). The amount of each isotope present in the samples was determined and this information was used to calculate the extracellular space and the intracellular concentration of 2-deoxyglucose. Rates of uptake were normalized to wet muscle mass in each vial.

2.11. Statistical methods

All data are reported as the mean ± standard deviation. Group mean values were compared by Student's two-tailed *t*-test. Results with *P*-values <0.05 were considered statistically significant.

3. Results

3.1. Activation of AMPK is reduced in oxidative muscle tissues of fasting TKO mice

We previously demonstrated that cardiac and skeletal muscle-specific Txnip KO mice recapitulated the metabolic phenotype of whole body Txnip KO mice [4]. Since AMPK is the major energy sensor orchestrating adaptive metabolic changes to fasting, we investigated if Txnip ablation would affect AMPK signaling in the heart and skeletal muscle. While total AMPKα protein level in TKO mice was the same as wild-type (WT) mice, activation of AMPKα through Thr-172 phosphorylation was markedly diminished in soleus and hearts of fasted TKO mice (Fig. 1A). In contrast, there was no difference in AMPK activation in soleus and hearts of non-fasted TKO mice, as compared to the WT controls (Fig. 1B). Interestingly, activation of AMPK was also not diminished in gastrocnemius from both fasted and non-fasted TKO mice (Fig. 1A
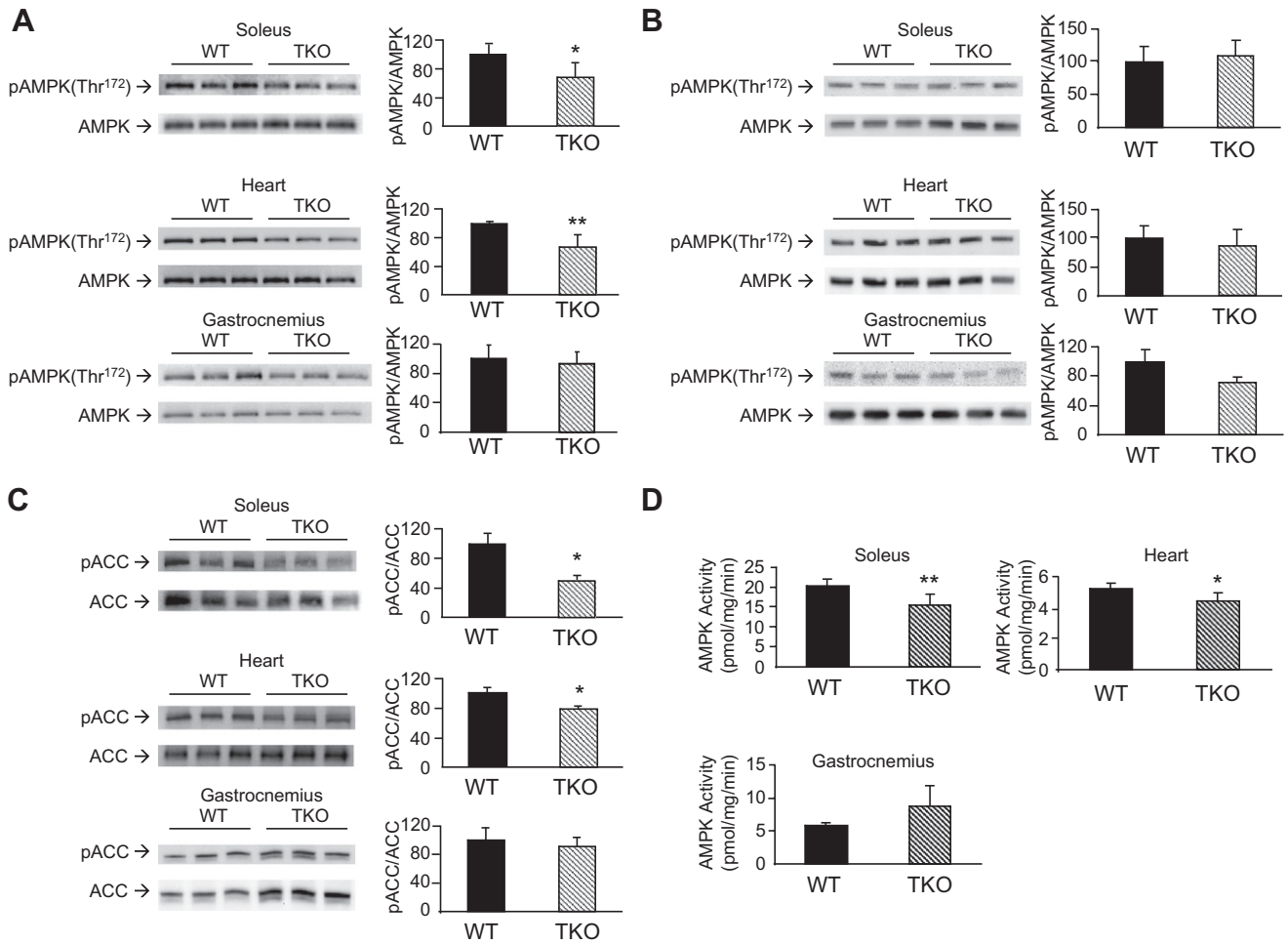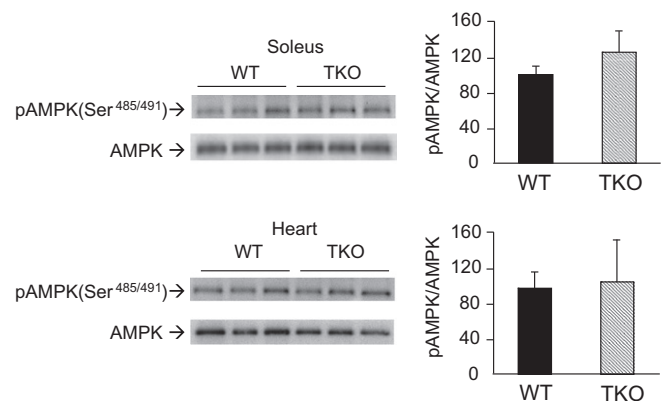
Fig. 1. Effects of Txnip ablation on AMPK activation and ACC phosphorylation. Tissue homogenates from soleus muscle and hearts were prepared from overnight fasted (A) and non-fasted (B) WT and TKO mice. Equal amounts of protein were resolved by SDS–PAGE. Levels of total AMPK and phospho-AMPKα (pThr-172) were quantified by Western blotting. Results are presented as mean ± S.D. from three mice in each group. (C) Phosphorylation levels of the AMPK downstream target ACC (pSer-79) and total ACC were determined by Western blotting. Results are presented as mean ± S.D. from three mice in each group. (D) AMPK enzyme activity was determined in homogenates from the heart, soleus and gastrocnemius muscles of fasted WT and TKO mice. Results are presented as mean ± S.D. from three mice in each group. $^*P < 0.05$ and $^{**}P < 0.01$ versus control mice.

and B). These findings suggest that Txnip ablation exerts different effects on oxidative muscles (soleus and cardiac muscle) than glycolytic muscles (gastrocnemius). Consistent with reduced AMPK activation, phosphorylation of acetyl-CoA carboxylase (ACC) at Ser-79, a downstream AMPK phosphorylation target, was also diminished in the fasting heart and soleus but not in gastrocnemius (Fig. 1C). The reduction in AMPK activation in fasting soleus and hearts was further confirmed by the decrease in AMPK activity measured in vitro (Fig. 1D).

### 3.2. Activation of AMPK by LKB1 and AMP are normal in TKO mice

TKO mice exhibit increased insulin sensitivity [4,19,20]. Phosphorylation of AMPK at Ser-485/491 (AMPKα) by the serine/threonine protein kinase B (Akt) is known to inhibit Thr-172 phosphorylation [21]. We examined if the decrease in AMPK activation could be due to cross-talk inhibition exerted by the insulin/Akt pathway through Ser-485/491 phosphorylation of AMPKα. No difference in Ser-485/491 phosphorylation levels between TKO mice and WT control mice was observed (Fig. 2). These data suggest that hypo-phosphorylation of AMPK at Thr-172 is unlikely due to the inhibitory action by Akt.

Since LKB1 is the major upstream kinase that phosphorylates AMPK in response to energy deprivation [22], we examined whether

Fig. 2. Effects of Txnip ablation on Ser-485/491 phosphorylation of AMPKα. Samples were prepared as in Fig. 1. Levels of pSer-485/491 in AMPKα in fasted soleus muscle and hearts were quantified. Results are presented as mean ± S.D. from three mice in each group.

ablation of Txnip may have affected the function of LKB1. TKO mice have similar expression levels of LKB1 as that of WT mice (Fig. 3A), indicating that Txnip ablation did not alter LKB1 protein expression.
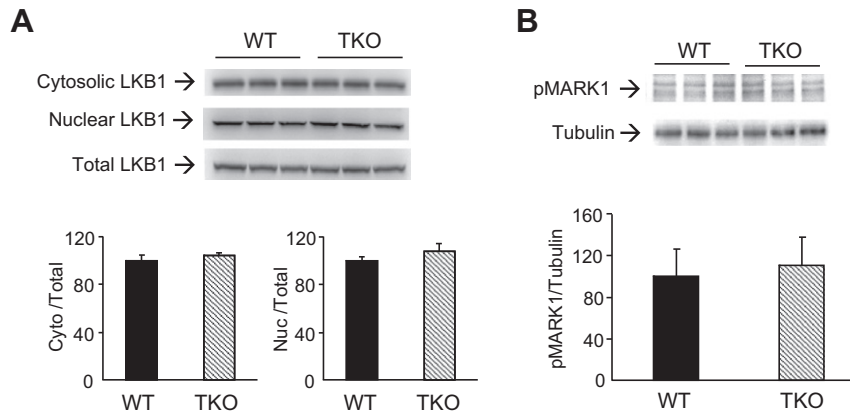
Fig. 3. Effects of Txnip ablation on LKB1 expression and function. (A) Tissue homogenate from soleus muscle of fasted mice was subfractionated into nuclear and cytosolic fractions. Ratios of cytosolic LKB1/total LKB1 and nuclear LKB1/total LKB1 were determined. (B) Levels of phospho-MARK1 (phosphorylation loop). Results are presented as mean ± S.D. (n = 3).

Nucleocytoplasmic transport and subsequent association of LKB1 with STE20-related adaptor protein (STRAD) and the scaffolding protein calcium binding protein 39 (CAB39) in the cytoplasm are required for full activation of LKB1 and AMPK [23]. Fig. 3A showed that cytosolic and nuclear distribution of LKB1 level was not altered in TKO mice. To confirm that LKB1 enzyme activity is not deficient in TKO mice, we examined the phosphorylation status of MAP/microtubule affinity-regulating kinase 1 (MARK1), another established LKB1 phosphorylation target. Fig. 3B showed that levels of MARK1 phosphorylation in TKO mice were the same as that of WT controls. Taken together, these findings showed that diminished activation of AMPK in fasting TKO mice is not due to LKB1 deficiency. We next examined if sensing of AMP by AMPK is defective in TKO mice. WT and TKO mice were treated with AICAR, an AMP analog which is metabolized to AICAR monophosphate (ZMP) mimicking the stimulatory effects of AMP on AMPK [24]. As expected, WT mice treated with AICAR exhibited a robust increase in Thr-172 phosphorylation of AMPK when compared to the saline-injected controls (Fig. 4). Interestingly, TKO mice were equally responsive to AICAR treatment

(Fig. 4), suggesting that the mechanism by which AMP activates AMPK is intact in TKO mice.

3.3. Txnip ablation alters cellular AMP:ATP ratio

Results from the AICAR stimulation experiment strongly suggest that intracellular AMP levels may explain the difference in AMPK activation. Levels of cellular adenosine nucleotides in tissues from fasted WT and TKO mice were quantified by LC/MS (Table 1). In both soleus and hearts, AMP levels in TKO mice were significantly reduced compared to WT mice (70.7% and 32.0%, P = 0.002 and 0.006, respectively). Consistent with the finding that AMPK phosphorylation was not affected in gastrocnemius, AMP level in gastrocnemius from fasted TKO mice was not different from that of WT controls. Fasting ATP level in soleus and gastrocnemius of TKO mice were both elevated (14.4%, P = 0.037 and 21.8%, P = 0.0001, respectively), whereas it was reduced in the heart (9.7%, P = 0.001). AMP:ATP ratio was lower in all three tissues of TKO mice: soleus (74.5%, P = 0.002), hearts (24.6%, P = 0.034) and gastrocnemius (20.8%, P = 0.005). Taken together, these data showed that diminished AMPK activation in fasting TKO soleus and hearts is not due to deficiencies in upstream kinase function or the capability of AMP to stimulate AMPK, but rather a consequence of decreased cellular AMP levels.
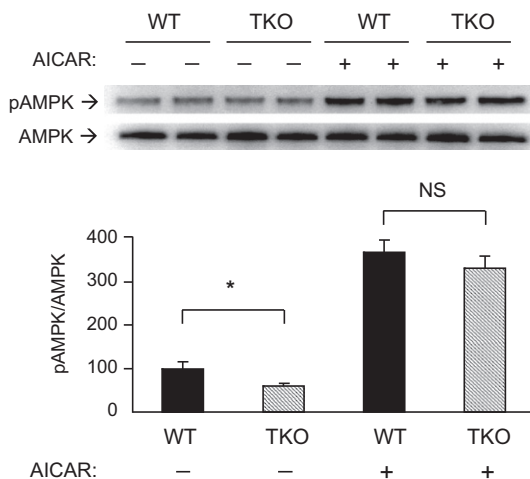
Fig. 4. Induction of AMPK phosphorylation by AICAR. Overnight fasted WT and TKO mice (n = 3 per group) were injected (s.c.) with saline or AICAR (0.5 mg/g). One hour after the treatment, soleus muscle was harvested. Levels of total AMPK and phospho-AMPKα (Thr-172) were determined by Western blot analysis. A representative blot is shown using duplicate samples from each group. Results are presented as mean ± S.D. *P < 0.05 and NS denotes no significant difference versus WT.

Table 1
Quantitative analysis of cellular adenosine nucleotides in fasted mice by LC/MS.

	n	AMP (μmol/g tissue)	ADP (μmol/g tissue)	ATP (μmol/g tissue)	AMP:ATP
Soleus (fasting)					
WT	9	0.318 ± 0.154	0.632 ± 0.090	9.297 ± 1.010	0.034 ± 0.017
TKO	8	0.093 ± 0.021	0.587 ± 0.050	10.635 ± 1.325	0.009 ± 0.002
P		0.002	0.221	0.037	0.002
Heart (fasting)					
WT	10	6.529 ± 1.732	0.654 ± 0.097	7.066 ± 0.392	0.927 ± 0.253
TKO	10	4.440 ± 1.108	0.631 ± 0.054	6.379 ± 0.338	0.699 ± 0.183
P		0.006	0.526	<0.001	0.034
Gastrocnemius (fasting)					
WT	10	0.206 ± 0.022	0.471 ± 0.044	7.158 ± 0.757	0.029 ± 0.004
TKO	10	0.201 ± 0.039	0.564 ± 0.041	8.719 ± 0.334	0.023 ± 0.004
P		0.707	<0.001	<0.001	0.005

Cellular adenosine nucleotides in overnight fasted WT and TKO mice. Levels of AMP, ADP and ATP in tissue extracts were determined by LC/MS. Normalized results are presented as mean ± S.D. P values (WT versus TKO) are presented.

3.4. Increased glucose utilization in muscle tissues of TKO mice is not associated with glucose transporter expression

One of the key functions of AMPK is to increase glucose uptake and utilization in response to energy deprivation. Paradoxically, we found that both glucose uptake and glycolysis were elevated in fasting TKO mice [4] despite having blunted AMPK activation (Fig. 1). Plasma levels of insulin in fasting TKO mice are the same as that of WT mice, whereas insulin levels of non-fasting TKO mice are lower than that of WT mice (Fig. 5A). Soleus isolated from fasting TKO mice showed increased 2-deoxyglucose uptake in the absence of insulin (Fig. 5B). This finding is consistent with those of Patwari et al. who showed that overexpression of Txnip in cultured 3T3-L1 adipocytes reduced 2-deoxyglucose uptake in the absence of insulin [13].

We examined if Txnip ablation alters the expression of glucose transporters GLUT4 and GLUT1. Heart tissues from WT and TKO mice were subfractionated. Purity and enrichment of plasma membrane was assessed by the presence of the cell surface marker β1-integrin (Fig. 6A, top panel). Induction of GLUT4 expression in plasma membrane samples from AICAR-stimulated WT mice served as positive controls (Fig. 6A, top panel). No difference was observed in the abundance of GLUT4 protein on the plasma membrane between TKO and WT mice (Fig. 6A, bottom panel). Unexpectedly, GLUT1 protein levels in the heart, soleus and gastrocnemius were lower in fasted TKO mice (Fig. 6B); however, no difference was observed in non-fasted animals (Fig. 6C). Parallel to the fasting GLUT1 protein difference, GLUT1 mRNA expression was diminished in fasted TKO mice, suggesting that the reduction in GLUT1 protein levels is due to transcriptional down-regulation (Fig. 6D). Since GLUT1 mRNA levels were reduced in gastrocnemius despite the absence of impairment in AMPK activation, these findings indicate the down-regulation of GLUT1 expression by Txnip ablation acts through a mechanism independent to AMPK signaling.
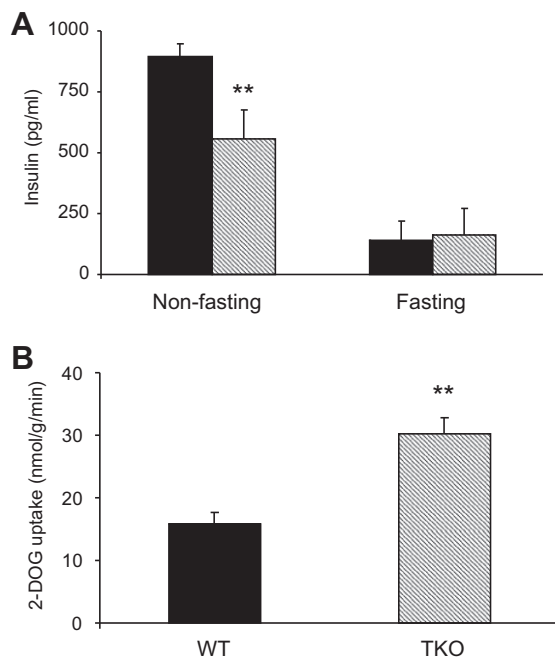
3.5. Txnip ablation induces inhibition of the mitochondrial pyruvate dehydrogenase complex, and is associated with increased muscle glycogen content

High energy state (low AMP:ATP ratio) activates pyruvate dehydrogenase kinases (PDKs) [25] which in turn phosphorylates and inhibits pyruvate dehydrogenase (PDH) [26]. Phosphorylation levels of the PDH-E1α subunit was markedly increased in soleus muscle from fasting TKO mice (Fig. 7A), whereas no difference was observed in non-fasted mice ($P = 0.07$, Fig. 7B). This finding is consistent with our previous data showing that glucose oxidation was diminished, whereas lactate production and glycolysis were increased in fasted TKO soleus muscles [4].
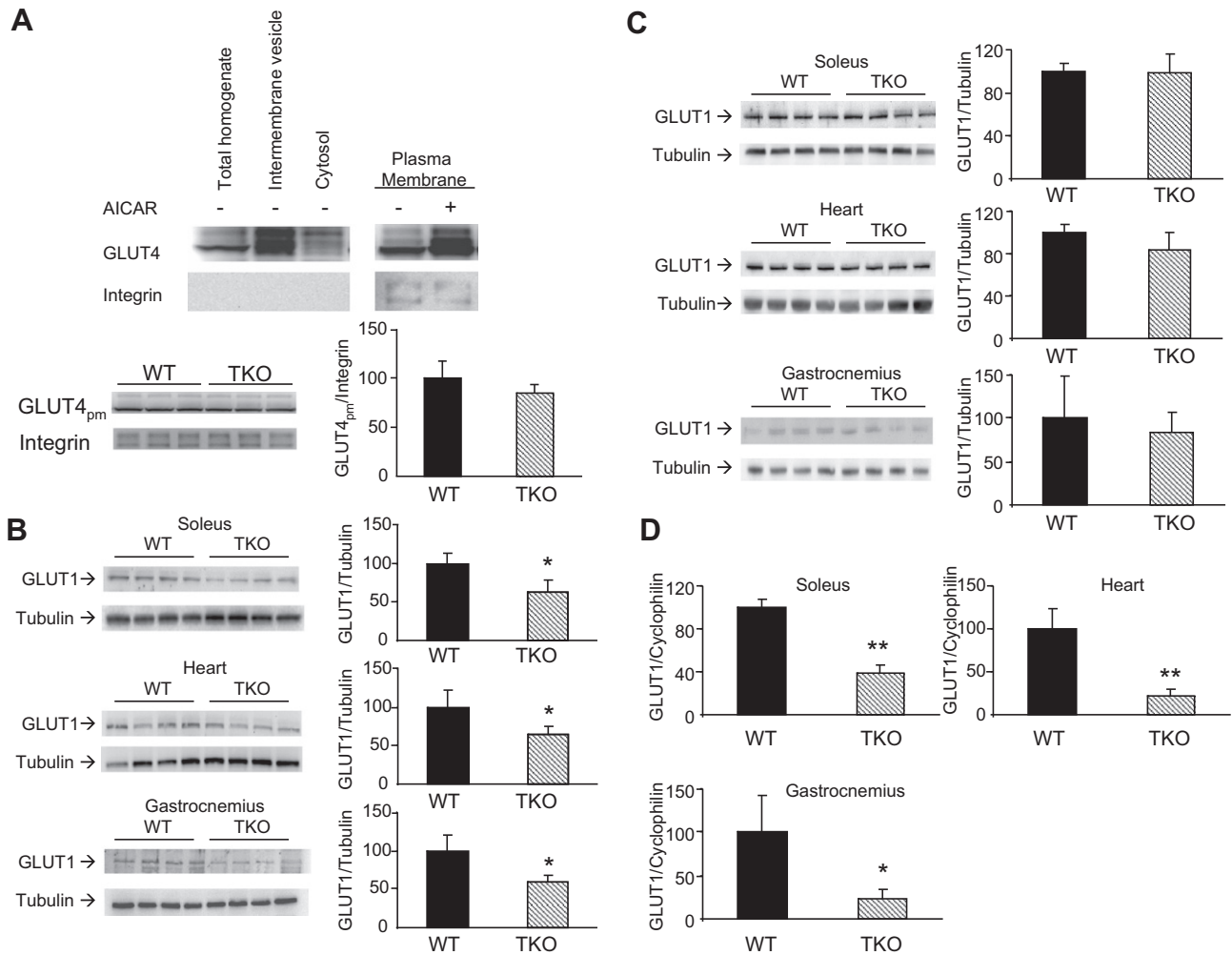
Glycogen content in the heart and soleus of fasted TKO mice were dramatically increased (5.6-fold and 5.3-fold, respectively, Fig. 8A). In non-fasted animals, a trend towards increased glycogen content in the hearts and soleus of TKO mice versus WT controls was observed, but did not reach statistical significance ($P = 0.21$ and 0.06, respectively, Fig. 8B). In contrast, glycogen content in the gastrocnemius of fasted and non-fasted TKO mice were not increased comparing to WT controls (Fig. 8A and B).

4. Discussion

Negative feedback mechanisms provide fail-safe measures to regain homeostasis in biological systems. In the case of counteracting energy deprivation (as in fasting and impaired mitochondrial oxidation), AMPK senses the decline in cellular energy status and coordinately modifies metabolic pathways to increase ATP production [14]. Activation of mitochondrial fatty acid oxidation by AMPK signaling in skeletal muscle provides a means to spare glucose for the brain, which relies on glucose as the major source of energy during acute fasting [27]. We previously showed that mitochondrial oxidation of glucose, fatty acids and ketone bodies were reduced in fasted TKO mice [4]. In this study, we further characterized the metabolic consequences of Txnip ablation and show for the first time that AMPK activation is blunted in the heart and soleus muscle, but not gastrocnemius muscle, of fasted TKO mice (Fig. 1A). The reduction in AMPK activation is associated with a decrease in cellular levels of AMP. This change is specific to tissues enriched in oxidative fibers (heart and soleus muscle) but not in those high in glycolytic fibers (gastrocnemius) (Table 1). The fact that gastrocnemius muscle has a high capacity of glycolysis may explain why it is less susceptible to the effect of impaired mitochondrial oxidation and increased glucose uptake caused by Txnip deficiency. In contrary, cardiac and soleus muscles contain more oxidative fibers and thus are more reliant on mitochondrial oxidation. As a result, the surplus glucose influx is channeled into glycogen storage. This is supported by our finding that glycogen accumulates in heart and soleus of fasting TKO mice but not in gastrocnemius (Fig. 8).

Despite having impaired mitochondrial fuel oxidation, we made a surprising finding that tissues of fasted TKO mice were in a paradoxically higher energetic state (Table 1). As glucose oxidation is impaired in TKO mice, the paradoxical finding of an elevated energy state in fasted TKO mice could be attributed, at least in part, to the increase in glycolysis as previously reported [4]. Reduced AMP:ATP ratio favors the phosphorylation and inhibition of PDH through the activation of PDKs. Forced expression of PDK1 in hypoxic HIF-1α null cells has been shown to increase ATP levels and shunt glucose metabolites from the mitochondria to glycolysis [28].

It is presently unclear how Txnip ablation leads to increased glucose uptake. Fasting insulin levels of TKO mice were not different from WT mice (Fig. 5A). Although fasted TKO mice have been

Fig. 5. Plasma insulin levels and 2-deoxyglucose uptake. (A) Plasma insulin levels in fasted and non-fasted WT (filled bars) and TKO (hatched bars) mice. Results are presented as mean ± S.D. ($n = 4$). (B) 2-Deoxyglucoe uptake by soleus isolated from fasted WT and TKO mice. Results are presented as mean ± S.D. ($n = 3$). **$P < 0.01$ versus control mice.

Fig. 6. Effects of Txnip ablation on GLUT1 and GLUT4 expression. (A) Top panel, heart homogenate from overnight fasted WT mice was subfractionated to obtain enriched plasma membranes, intermembrane vesicles and cytosolic fractions for Western blot analysis. Thirty micrograms of protein from each fraction was resolved by SDS–PAGE. Bottom panel, GLUT4 expression in plasma membrane of hearts from overnight fasted WT and TKO mice. (B and C) Levels of GLUT1 protein in fasted (B) and non-fasted (C) mice. Results are presented as mean ± S.D. ($n = 4$). (D) Relative expression of GLUT1 mRNA in the heart, soleus and gastrocnemius muscles of fasted WT and TKO mice. Results are presented as mean ± S.D. ($n = 5$). *$P < 0.05$ and **$P < 0.01$ versus control mice.
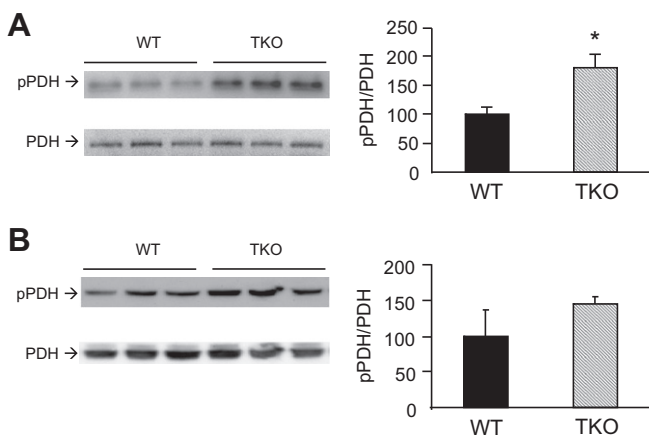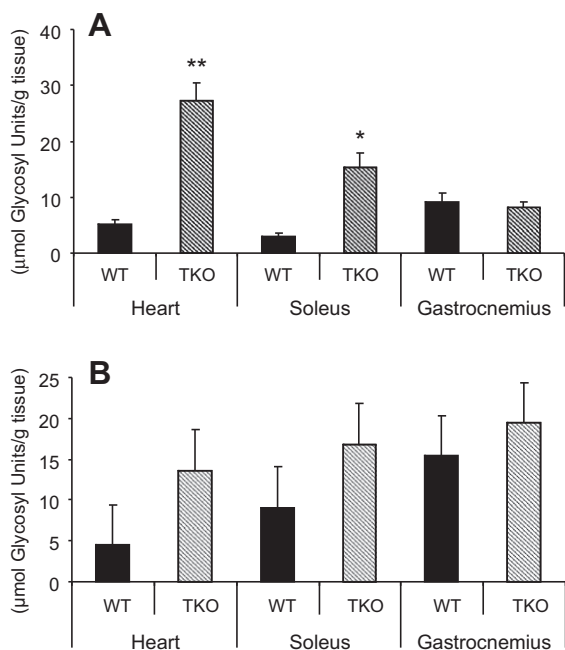

Fig. 7. Effects of Txnip ablation on pyruvate dehydrogenase. Levels of phospho-pyruvate dehydrogenase (pSer-293 of PDH-E1α) in soleus muscles from overnight fasted (A) and non-fasted (B) WT and TKO mice were determined. Results are presented as mean ± S.D. ($n = 3$). *$P < 0.05$ versus control mice.

shown to have increased insulin sensitivity [4,20], we did not observe any increase in GLUT4 translocation to the plasma

membrane in TKO hearts (Fig. 6A). This may be attributed to the reduced AMPK signaling in TKO hearts which leads to decreased phosphorylation of Akt substrate of 160 kDa (AS160) and GLUT4 translocation [29]. Uptake of 2-deoxyglucose in the absence of insulin by isolated soleus from fasting TKO mice was increased comparing to WT controls (Fig. 5B). In accordance with findings from overexpression studies of Txnip in cultured adipocytes [13], our data suggest that increased uptake of glucose in muscle is likely mediated by an insulin-independent mechanism. Previously, we showed that streptozotocin treatment normalized plasma triglyceride levels in Txnip null HcB-19 mice and led to hyperglycemia in both control and HcB-19 mice. The seemingly contradicting findings on the role of insulin in these two studies can be reconciled by the fact that insulin affects glucose secretion by the liver but not glucose uptake in the muscle. Absence of insulin in streptozotocin-treated mice suppresses hepatic lipoprotein and leads to uncontrolled hepatic glucose output.

Despite have increased glucose uptake, GLUT1 protein expression was unexpectedly lower in fasting TKO mice, whereas no difference was observed in non-fasting animals (Fig. 6B and C). The down-regulation of GLUT1 transcription appears to be independent to AMPK as GLUT1 expression in gastrocnemius from fasting TKO mice was also reduced (Fig. 6D). The role of Txnip in

Fig. 8. Effects of Txnip ablation on glycogen content. Glycogen content in the heart, soleus and gastrocnemius muscles from fasting (A) and non-fasting (B) WT and TKO mice. Results are presented as mean ± S.D. ($n = 3$). $*P < 0.05$ and $**P < 0.01$ versus control mice.

regulating GLUT1 remains to be elucidated. However, our data indicate that modulation of glucose uptake by Txnip does not involve increased recruitment of the two most abundant glucose transporters, namely GLUT1 and GLUT4, in the muscle. Mutagenesis studies demonstrated that modulation of glucose uptake by Txnip in cultured cells was independent of its ability to bind thioredoxin-1 and that regulation of glucose uptake was intrinsic to the arrestin-like domain in Txnip [13]. This raised the possibility that Txnip might act as a scaffold protein facilitating the interactions between other regulatory proteins of glucose metabolism. For example, it was discovered that Txnip interacts with NLRP3 and plays an essential role in regulating inflammasome activities [30]. Interestingly, NLRP3 knockout mice also exhibited increased glucose tolerance and insulin sensitivity similar to the phenotype of TKO mice, suggesting that the inflammasome pathway could be linked to the regulation of glucose homeostasis by Txnip [30]. Although the present study cannot exclude the possibility of alterations in other hexose transporters and their kinetic properties, a plausible explanation for the increase in glucose uptake without apparent increase in GLUT1 and GLUT4 expression could be, in part, due to increased rate of glycolysis [4] and the diversion of glucose metabolites to glycogen storage (Fig. 8).

McBride et al. demonstrated that glycogen inhibited AMPK activity in a highly purified cell-free system [31]. AMPK associates with glycogen synthase and glycogen phosphorylase in skeletal muscle [32]. The β subunits of AMPK contain a central conserved glycogen-binding domain which mediates the association between AMPK and glycogen. These findings suggest that AMPK may monitor the level of cellular energy reserve in the form of glycogen, in addition to its well-established role as immediate energy sensor of the AMP:ATP ratio. Physiological studies also showed that muscle AMPK activity is modulated by glycogen content [33,34]; however, the underlying mechanisms are poorly understood. Glycogen depleted muscle exhibits greater AMPK activation by AICAR treatment or by exercise, whereas glycogen loading represses AMPK activation [33,34]. In fasted TKO mice, cellular glycogen content was found to be dramatically increased in soleus and hearts (Fig. 8). This is in line with data from hyperinsulinemic–euglycemic clamp studies showing that whole body rates of glycolytic and glycogen synthesis were significantly elevated in TKO mice [35]. The increased glycogen content, in addition to the observed decrease in AMP levels, may further attenuate AMPK activation. Similar to the metabolic phenotype of TKO mice, increased plasma lactate levels and muscle glycogen content are associated with human mitochondrial insufficiency disorders [36–38].

Txnip is intimately linked to cellular carbohydrate and mitochondrial metabolism through the glucose sensing transcriptional complex MondoA:Mlx [39–41]. Increased glycolytic flux downregulates Txnip gene expression [41]. Induction of Txnip by lactic acidosis acts as a feedback mechanism to reduce glucose uptake and lactate production, whereas this protective measure is blunted in Txnip deficient cells [40]. In addition to promoting mitochondrial oxidation to generate ATP from fatty acid and ketone bodies oxidation, AMPK reduces the deleterious effects of lactic acidosis. Activation of AMPK in skeletal muscle induces the expression of monocarboxylate transporter-4 [42], which is the predominant transporter for lactate efflux. The inability of TKO mice to upregulate Txnip and activate AMPK pathway could reduce the tolerance to lactic acidosis and contribute to the increased mortality during long term fasting. Glucose sparing by skeletal muscles during fasting is a crucial evolutionary adaption to survival since the brain can only utilize glucose as energy source during early stage of starvation. Our studies highlight the indispensible role of Txnip in maintaining glucose homeostasis and adapting to starvation through AMPK signaling.

Acknowledgements

References

[1] Bodnar, J.S., Chatterjee, A., Castellani, L.W., Ross, D.A., Ohmen, J., Cavalcoli, J., Wu, C., Dains, K.M., Catanese, J., Chu, M., Sheth, S.S., Charugundla, K., Demant, P., West, D.B., de Jong, P. and Lusis, A.J. (2002) Positional cloning of the combined hyperlipidemia gene Hyplip1. Nat. Genet. 30, 110–116.

[2] Chutkow, W.A., Patwari, P., Yoshioka, J. and Lee, R.T. (2008) Thioredoxin-interacting protein (Txnip) is a critical regulator of hepatic glucose production. J. Biol. Chem. 283, 2397–2406.

[3] Oka, S., Liu, W., Masutani, H., Hirata, H., Shinkai, Y., Yamada, S., Yoshida, T., Nakamura, H. and Yodoi, J. (2006) Impaired fatty acid utilization in thioredoxin binding protein-2 (TBP-2)-deficient mice: a unique animal model of Reye syndrome. FASEB J. 20, 121–123.

[4] Hui, S.T., Andres, A.M., Miller, A.K., Spann, N.J., Potter, D.W., Post, N.M., Chen, A.Z., Sachithanantham, S., Jung, D.Y., Kim, J.K. and Davis, R.A. (2008) Txnip balances metabolic and growth signaling via PTEN disulfide reduction. Proc. Natl. Acad. Sci. USA 105, 3921–3926.

[5] Hui, T.Y., Sheth, S.S., Diffley, J.M., Potter, D.W., Lusis, A.J., Attie, A.D. and Davis, R.A. (2004) Mice lacking thioredoxin-interacting protein provide evidence linking cellular redox state to appropriate response to nutritional signals. J. Biol. Chem. 279, 24387–24393.

[6] Nishiyama, A., Matsui, M., Iwata, S., Hirota, K., Masutani, H., Nakamura, H., Takagi, Y., Sono, H., Gon, Y. and Yodoi, J. (1999) Identification of thioredoxin-binding protein-2/vitamin D(3) up-regulated protein 1 as a negative regulator of thioredoxin function and expression. J. Biol. Chem. 274, 21645–21650.

[7] Patwari, P., Higgins, L.J., Chutkow, W.A., Yoshioka, J. and Lee, R.T. (2006) The interaction of thioredoxin with Txnip. Evidence for formation of a mixed disulfide by disulfide exchange. J. Biol. Chem. 281, 21884–21891.

[8] Parikh, H., Carlsson, E., Chutkow, W.A., Johansson, L.E., Storgaard, H., Poulsen, P., Saxena, R., Ladd, C., Schulze, P.C., Mazzini, M.J., Jensen, C.B., Krook, A.,

Bjornholm, Y., Tornqvist, H., Zierath, J.R., Ridderstrale, M., Altshuler, D., Lee, R.T., Vaag, A., Groop, L.C. and Mootha, V.K. (2010) TXNIP regulates peripheral glucose metabolism in humans. PLoS Med. 4, e158.

[9] Sheth, S.S., Castellani, L.W., Chari, S., Wagg, C., Thipphavong, C.K., Bodnar, J.S., Tontonoz, P., Attie, A.D., Lopaschuk, G.D. and Lusis, A.J. (2005) Thioredoxin-interacting protein deficiency disrupts the fasting-feeding metabolic transition. J. Lipid Res. 46, 123–134.

[10] Hirota, T., Okano, T., Kokame, K., Shirotani-Ikejima, H., Miyata, T. and Fukada, Y. (2002) Glucose down-regulates Per1 and Per2 mRNA levels and induces circadian gene expression in cultured Rat-1 fibroblasts. J. Biol. Chem. 277, 44244–44251.

[11] Shalev, A., Pise-Masison, C.A., Radonovich, M., Hoffmann, S.C., Hirshberg, B., Brady, J.N. and Harlan, D.M. (2002) Oligonucleotide microarray analysis of intact human pancreatic islets: identification of glucose-responsive genes and a highly regulated TGFbeta signaling pathway. Endocrinology 143, 3695–3698.

[12] Pang, S.T., Hsieh, W.C., Chuang, C.K., Chao, C.H., Weng, W.H. and Juang, H.H. (2009) Thioredoxin-interacting protein: an oxidative stress-related gene is upregulated by glucose in human prostate carcinoma cells. J. Mol. Endocrinol. 42, 205–214.

[13] Patwari, P., Chutkow, W.A., Cummings, K., Verstraeten, V.L., Lammerding, J., Schreiter, E.R. and Lee, R.T. (2009) Thioredoxin-independent regulation of metabolism by the alpha-arrestin proteins. J. Biol. Chem. 284, 24996–25003.

[14] Towler, M.C. and Hardie, D.G. (2007) AMP-activated protein kinase in metabolic control and insulin signaling. Circ. Res. 100, 328–341.

[15] Derave, W., Ai, H., Ihlemann, J., Witters, L.A., Kristiansen, S., Richter, E.A. and Ploug, T. (2000) Dissociation of AMP-activated protein kinase activation and glucose transport in contracting slow-twitch muscle. Diabetes 49, 1281–1287.

[16] Vitorino, R., Ferreira, R., Neuparth, M., Guedes, S., Williams, J., Tomer, K.B., Domingues, P.M., Appell, H.J., Duarte, J.A. and Amado, F.M. (2007) Subcellular proteomics of mice gastrocnemius and soleus muscles. Anal. Biochem. 366, 156–169.

[17] Zhou, M., Sevilla, L., Vallega, G., Chen, P., Palacin, M., Zorzano, A., Pilch, P.F. and Kandror, K.V. (1998) Insulin-dependent protein trafficking in skeletal muscle cells. Am. J. Physiol. 275, E187–E196.

[18] Hansen, P.A., Gulve, E.A. and Holloszy, J.O. (1994) Suitability of 2-deoxyglucose for in vitro measurement of glucose transport activity in skeletal muscle. J. Appl. Physiol. 76, 979–985.

[19] Oka, S., Masutani, H., Liu, W., Horita, H., Wang, D., Kizaka-Kondoh, S. and Yodoi, J. (2006) Thioredoxin-binding protein-2-like inducible membrane protein is a novel vitamin D3 and peroxisome proliferator-activated receptor (PPAR)gamma ligand target protein that regulates PPARgamma signaling. Endocrinology 147, 733–743.

[20] Yoshihara, E., Fujimoto, S., Inagaki, N., Okawa, K., Masaki, S., Yodoi, J. and Masutani, H. (2010) Disruption of TBP-2 ameliorates insulin sensitivity and secretion without affecting obesity. Nat. Commun. 1, 127.

[21] Soltys, C.L., Kovacic, S. and Dyck, J.R. (2006) Activation of cardiac AMP-activated protein kinase by LKB1 expression or chemical hypoxia is blunted by increased Akt activity. Am. J. Physiol. Heart Circ. Physiol. 290, H2472–H2479.

[22] Shaw, R.J., Kosmatka, M., Bardeesy, N., Hurley, R.L., Witters, L.A., DePinho, R.A. and Cantley, L.C. (2004) The tumor suppressor LKB1 kinase directly activates AMP-activated kinase and regulates apoptosis in response to energy stress. Proc. Natl. Acad. Sci. USA 101, 3329–3335.

[23] Xie, Z., Dong, Y., Zhang, J., Scholz, R., Neumann, D. and Zou, M.H. (2009) Identification of the serine 307 of LKB1 as a novel phosphorylation site essential for its nucleocytoplasmic transport and endothelial cell angiogenesis. Mol. Cell. Biol. 29, 3582–3596.

[24] Hardie, D.G., Carling, D. and Carlson, M. (1998) The AMP-activated/SNF1 protein kinase subfamily: metabolic sensors of the eukaryotic cell? Annu. Rev. Biochem. 67, 821–855.

[25] Harris, R.A., Bowker-Kinley, M.M., Huang, B. and Wu, P. (2002) Regulation of the activity of the pyruvate dehydrogenase complex. Adv. Enzyme Regul. 42, 249–259.

[26] Hue, L. and Taegtmeyer, H. (2009) The randle cycle revisited: a new head for an old hat. Am. J. Physiol. Endocrinol. Metab. 297, E578–E591.

[27] Koh, H.J., Brandauer, J. and Goodyear, L.J. (2008) LKB1 and AMPK and the regulation of skeletal muscle metabolism. Curr. Opin. Clin. Nutr. Metab. Care 11, 227–232.

[28] Kim, J.W., Tchernyshyov, I., Semenza, G.L. and Dang, C.V. (2006) HIF-1-mediated expression of pyruvate dehydrogenase kinase: a metabolic switch required for cellular adaptation to hypoxia. Cell Metab. 3, 177–185.

[29] Yuasa, T. et al. (2009) The Rab GTPase-activating protein AS160 as a common regulator of insulin- and Galphaq-mediated intracellular GLUT4 vesicle distribution. Endocr. J. 56, 345–359.

[30] Zhou, R., Tardivel, A., Thorens, B., Choi, I. and Tschopp, J. (2010) Thioredoxin-interacting protein links oxidative stress to inflammasome activation. Nat. Immunol. 11, 136–140.

[31] McBride, A., Ghilagaber, S., Nikolaev, A. and Hardie, D.G. (2009) The glycogen-binding domain on the AMPK beta subunit allows the kinase to act as a glycogen sensor. Cell Metab. 9, 23–34.

[32] Chen, Z., Heierhorst, J., Mann, R.J., Mitchelhill, K.I., Michell, B.J., Witters, L.A., Lynch, G.S., Kemp, B.E. and Stapleton, D. (1999) Expression of the AMP-activated protein kinase beta1 and beta2 subunits in skeletal muscle. FEBS Lett. 460, 343–348.

[33] Wojtaszewski, J.F., MacDonald, C., Nielsen, J.N., Hellsten, Y., Hardie, D.G., Kemp, B.E., Kiens, B. and Richter, E.A. (2003) Regulation of 5′AMP-activated protein kinase activity and substrate utilization in exercising human skeletal muscle. Am. J. Physiol. Endocrinol. Metab. 284, E813–E822.

[34] Wojtaszewski, J.F., Jorgensen, S.B., Hellsten, Y., Hardie, D.G. and Richter, E.A. (2002) Glycogen-dependent effects of 5-aminoimidazole-4-carboxamide (AICA)-riboside on AMP-activated protein kinase and glycogen synthase activities in rat skeletal muscle. Diabetes 51, 284–292.

[35] Chutkow, W.A., Birkenfeld, A.L., Brown, J.D., Lee, H.Y., Frederick, D.W., Yoshioka, J., Patwari, P., Kursawe, R., Cushman, S.W., Plutzky, J., Shulman, G.I., Samuel, V.T. and Lee, R.T. (2010) Deletion of the {alpha}-arrestin protein Txnip in mice promotes adiposity and adipogenesis while preserving insulin sensitivity. Diabetes 59, 1424–1434.

[36] Horvath, R., Kemp, J.P., Tuppen, H.A., Hudson, G., Oldfors, A., Marie, S.K., Moslemi, A.R., Servidei, S., Holme, E., Shanske, S., Kollberg, G., Jayakar, P., Pyle, A., Marks, H.M., Holinski-Feder, E., Scavina, M., Walter, M.C., Coku, J., Gunther-Scholz, A., Smith, P.M., McFarland, R., Chrzanowska-Lightowlers, Z.M., Lightowlers, R.N., Hirano, M., Lochmuller, H., Taylor, R.W., Chinnery, P.F., Tulinius, M. and DiMauro, S. (2009) Molecular basis of infantile reversible cytochrome c oxidase deficiency myopathy. Brain 132, 3165–3174.

[37] Roodhooft, A.M., Van Acker, K.J., Martin, J.J., Ceuterick, C., Scholte, H.R. and Luyt-Houwen, I.E. (1986) Benign mitochondrial myopathy with deficiency of NADH-CoQ reductase and cytochrome c oxidase. Neuropediatrics 17, 221–226.

[38] Valente, L., Tiranti, V., Marsano, R.M., Malfatti, E., Fernandez-Vizarra, E., Donnini, C., Mereghetti, P., De Gioia, L., Burlina, A., Castellan, C., Comi, G.P., Savasta, S., Ferrero, I. and Zeviani, M. (2007) Infantile encephalopathy and defective mitochondrial DNA translation in patients with mutations of mitochondrial elongation factors EFG1 and EFTu. Am. J. Hum. Genet. 80, 44–58.

[39] Stoltzman, C.A., Peterson, C.W., Breen, K.T., Muoio, D.M., Billin, A.N. and Ayer, D.E. (2008) Glucose sensing by MondoA:Mlx complexes: a role for hexokinases and direct regulation of thioredoxin-interacting protein expression. Proc. Natl. Acad. Sci. USA 105, 6912–6917.

[40] Chen, J.L., Merl, D., Peterson, C.W., Wu, J., Liu, P.Y., Yin, H., Muoio, D.M., Ayer, D.E., West, M. and Chi, J.T. (2010) Lactic acidosis triggers starvation response with paradoxical induction of TXNIP through MondoA. PLoS Genet. 6.

[41] Yu, F.X., Chai, T.F., He, H., Hagen, T. and Luo, Y. (2010) Thioredoxin-interacting protein (Txnip) gene expression: sensing oxidative phosphorylation status and glycolytic rate. J. Biol. Chem. 285, 25822–25830.

[42] Furugen, A., Kobayashi, M., Narumi, K., Watanabe, M., Otake, S., Itagaki, S. and Iseki, K. (2011) AMP-activated protein kinase regulates the expression of monocarboxylate transporter 4 in skeletal muscle. Life Sci. 88, 163–168.